

ATMOSPHERIC EFFECTS REMOVAL OF ASAR-DERIVED INSAR PRODUCTS USING MERIS DATA AND GPS

S. Adham Khiabani^a, M. J. Valadan Zoej^a, M. R. Mobasheri^a, M. Dehghani^a

Geodesy and Geomatics Engineering Faculty, K.N.Toosi University of Technology, No. 1346,
Vali_Asr St., Tehran, Iran, Postcode: 1996715433
sina_adham@yahoo.com, valadanzouj@kntu.ac.ir, mobasheri@kntu.ac.ir, dehghani_rsgsi@yahoo.com_

WG I/2: SAR and LiDAR systems

KEY WORDS: Satellite remote sensing, Calibration, Interferometric SAR (InSAR), Spatial modeling, Atmosphere, Water vapor, MERIS

ABSTRACT:

As confirmed by many scientists, atmosphere has intensive contaminative role on Interferometric Synthetic Aperture Radar (InSAR) measurements. Atmospheric parameters, always influence radar's phase but the intensity of the atmospheric errors on interferograms depend on the difference of the parameters' values. In this paper, some calibration methods will be considered in order to reduce the errors in some scenes acquired in 2005 from Mashhad in North East of Iran which is a semi mountainous area. Therefore, model estimations and data acquiring processes were determined to sustain the climate's requirements. Since we have used *Advanced synthetic aperture Radar* (ASAR) data for interferometry purpose, MERIS seemed to be an appropriate data source due to the exact similarity of the acquisition times of MERIS and ASAR. As water vapor products which derived from optical Spaceborn sensors are significantly sensitive to the clouds, a cloud mask algorithm was issued and an interpolation method was utilized to fill the empty pixels of the water vapor product. The air pressure and water vapor differential maps was formed in the next step and the derived differential maps was converted to zenith delay and radar phase shift respectively. As interferogram flattening was decided to be done after error removal process, the Ionospheric effect was neglected due to its linear influence in the area of interest. Implementing the model to the ASAR interferogram showed that the corrected InSAR results agreed to the independent GPS measurements with around a centimeter difference. Furthermore, atmospheric artifacts were significantly reduced in the final product.

1. INTRODUCTION

Interferometric Synthetic Aperture Radar (InSAR) has demonstrated its ability in measuring surface displacements (Massonnet et al., 1993; Zebker et al., 1994b) and topographic mapping (Zebker et al., 1994a). As confirmed by many scientists, atmosphere has an intensive contaminative role on *Interferometric Synthetic Aperture Radar* (InSAR) measurements (Zebker et. al, 1997). Atmospheric parameters, always influence radar's phase but, the intensity of the atmospheric errors on interferograms depend on the difference of the parameters' values (Hanssen, 2001). In the other words, a same atmospheric condition in two radar data times of acquisition may cause the minimum atmospheric error on derived interferogram due to the omission of the error, during the interferogram forming process (Zebker et. Al., 1997).

In the SAR interferometry, atmosphere parameters may cause a phase shift on the sensed signal (Hanssen, 2001). This phase shift would results in a mismeasurement in surface deformation estimation. A spatially linear changing parameter such as Ionospheric electron content (neglecting exceptions) or a parameter with a fixed horizontal gradient (Air pressure in stable conditions) will cause a fixed or almost fixed drift in deformation estimation (Hanssen, 2001). This effect is hard to separate with the Baseline effect. Implementing the flattening strategy after the atmospheric error reduction process may reduce this effect in addition.

The phase shift of the Radar signal depends on the changes of *Refractivity* in different air stratum. The refractivity could be obtained from the Eq.1 (Davis et al., 1985).

$$N = k_1 \frac{P}{T} + \left(k_2' \frac{e}{T} + k_3 \frac{e}{T^2} \right) - 4.028 \times 10^7 \frac{n_e}{f^2} + 1.45w \quad (1)$$

The first term of the equation is dry term, the next two terms in the brackets named wet term and the other terms are Ionospheric and liquid terms respectively (Hanssen, 2001).

As it could be seen in the Eq.1, refractivity is mainly under the influence of 5 parameters of Temperature, Air pressure, Partial pressure of water vapor, Ionospheric total electron content and liquid water content.

Water vapor effects have been introduced as the dominant error source of InSAR deformation products among the all kinds of atmospheric influences due to its common nonlinear spatial changes in a limited area (Hanssen, 2001; Li et. al, 2005).

Stacking and Calibration methods are two suggested strategies of atmospheric correction of InSAR products (Li et. al, 2005). Stacking methods include those strategies which are implemented to raw data to obtain better qualified derived products (Zebker et al., 1997). Whereas, the calibration methods are those which are implemented to the products to increase the accuracy of derived data (Li et al., 2005).

Some conventional implemented stacking methods showed that the derived data could obtain the acceptable accuracies (Zebker et al., 1997) but, the results are not ideal in most cases (Li et al., 2005). On the other hand, an extensive parametric model is needed to achieve higher accuracies due to the various atmospheric effects on the InSAR data. Furthermore, the model should be flexible enough to be extended for special cases.

In this paper, some calibration methods will be considered in order to reduce the errors in some scenes acquired in September and October of 2005 from Mashhad in North East of Iran which is a semi mountainous area. Therefore, model estimations and data acquiring processes were determined to sustain the climate's requirements.

In many cases, using a dense GPS network could be simple, accurate and appropriate for atmospheric modeling (Li et al., 2005). These kinds of networks are not available in the existing area of interest so, a calibrated spaceborn water vapor product was chosen as the next suitable choice due to its extensive coverage. Moreover, due to the smooth changes of atmospheric parameters, the resolution of the optical water vapor products is suitable either. Since we have used *Advanced Synthetic Aperture Radar* (ASAR) data for interferometry purpose, MERIS seemed to be an appropriate data source due to the exact similarity of the acquisition times of MERIS and ASAR. As water vapor products which derived from optical Spaceborn sensors are significantly sensitive to the clouds (Li et al., 2005; Hanssen, 2001), a cloud extraction algorithm was issued and an interpolation method was utilized to fill the empty pixels of the product. To recover these values, it is needed to have some information about the geometrical depth and the liquid water content of the clouds (Hanssen, 2001). As such data are difficult to obtain, a simple method was used to mask or repair data.

MERIS Air pressure is another data source which could be helpful for the atmospheric correction of InSAR data. This layer is appropriate for different weather condition of two acquisition times. In this study, due to the minute changes of air pressure gradient, synoptic data was used due to its better accuracy.

Ionospheric total electron content was the other critical parameter which influences the Radar single ray (Hanssen, 2001). As the changes of total electron content in the narrow area like the interested region of fine mode images of ASAR, is spatially mitigating, the difference error map of Ionosphere seems to be planar. This error plane is difficult to separate from the baseline effect of the interferogram (Hanssen, 2001). Hence, by applying the flattening strategy after the error reduction process, this error and some residuals of other errors may be reduced.

In this paper and in the next section, the characteristics of utilized MERIS images will be introduced. Then the details of error removal strategies will be considered and in the other session, the results and validation methods will be noted. A short discussion will be done at the end of this paper.

2. MERIS

MERIS (MEdium Resolution Imaging Spectrometer) is a useful optical sensor of European ENVISAT for ocean color and atmospheric studies (Kramer, 2002). The images of this sensor consist of 15 spectral bands in visible and near infrared regions of electromagnetic waves. MERIS image is an appropriate tool for atmosphere monitoring and extraction of atmospheric parameters (ESA, 2006). One of the most important capability

of these images is the column water vapor estimation (ESA, 2006).

To estimate the total precipitable water vapor content of the atmosphere in the earth-sensor direction, a quadratic model between the band 14 and 15 could be used. These two bands are suitable for water vapor estimation because one of them is a water absorption channel and the other one is a non absorbing band (Fischer and Bennartz, 1998). Moreover, closeness of these two bands in the spectral pattern will result in the small difference between the surface albedo in two channels.

The column water vapor content is calculated in level 2 data of MERIS. In this research the MERIS Reduced resolution product was chosen to form the error maps (ESA, 2006).

These dataset consists of extracted cloud features and column water vapor. The nominal spatial resolution of data is 1200 meter and the accuracy of water vapor amount is 20% (ESA, 2006).

3. ERROR REDUCTOION

An interferogram was formed from SLC images of ASAR. Two single phase images were acquired in May 30, 2005 and August 08, 2005 from north east of Iran. Forming method and noise reduction strategies result in an interferogram with pixel spacing of 90 meters.

5 main signals were taken into account in this research (Hanssen, 2001).

- 1- Topographic term
- 2- Deformation signal
- 3- Noise
- 4- Baseline phase ramp
- 5- Atmospheric term

In this research, Topographic term considered as the additional signal and as the first step, topographic effect was removed by using DEMs.

Deformation is the required signal and all the considered strategies attempt to maintain this signal.

Noise reduction strategies were utilized in forming the interferogram and the remained noise was neglected.

Two remained terms was considered simultaneously. As the baseline error and atmospheric effect is hard to separate (Hanssen, 2001), a plane fit algorithm was chosen to flatten the interferogram. This algorithm reduced the remained atmospheric errors and baseline phase ramp at once.

As some parameters like water vapor have a fixed term in its total error, flattening before error reduction will cause the removal of this fixed term. Implementing the error map after flattening may reduce the influences more than theirs real amount.

As a result, the influences divided into two categories. First category includes the nonlinear effects like water vapor and second one consists of linear effects. Depends on the weather condition, air pressure and Ionospheric electron content may categorize in first or second group.

In the two times of acquisition, the wind speed was low and approximately equal. This fact caused nearly same horizontal gradient in air pressure (Mobasheri, 2006). In addition, no extraordinary Ionospheric phenomenon was detected. So the change gradient of Ionospheric parameters could assume the same.

In order to above discussion, water vapor and liquid water are the remained factors to be considered. But as a test, the differential map of air pressure will also be considered.

Figure 1 illustrates a part of the formed interferogram. As it could be seen (in A), a brief subsidence signal exists in this area. GPS and geological data also detect the deformation in the centre of this image. But InSAR shows deformation signals in surrounding points of the subsidence area which is not detected by GPS and geological surveys. This inhomogeneous and somehow wave-shaped signal which has around 4 centimeter disagreement with GPS points could be formed due to the atmosphere. There is around of a few centimeter disagreement between GPS and InSAR in subsidence area even after the flattening of the InSAR image (Figure 2). This is the motivation of the test of atmospheric correction strategies.

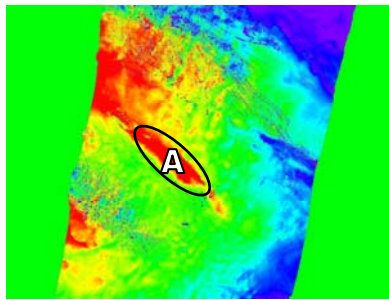


Figure1: Raw interferogram

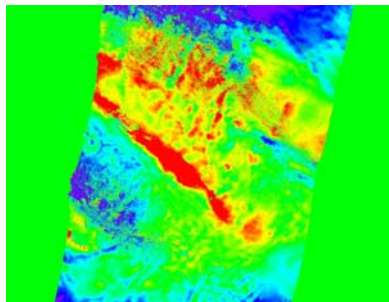


Figure2: Flattened Interferogram

Cloudy pixels cause a very low reflectance in the 14th band of MERIS and this results in an approximately zero-estimation in water vapor map. On the other hand, over cloud vapor estimations are not acceptable due to the high influential under clouds water vapor (Mobasheri, 2006). Interpolation could be an appropriate solution for this problem (Li et al., 2005).

A part of cloudy water vapor scene, acquired in 12th of September could be seen with the corresponding cloud extracted map in Figure3.

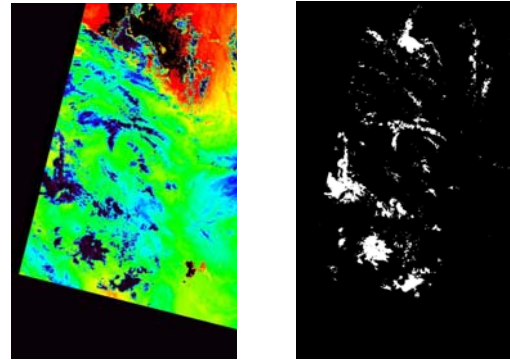


Figure3: Cloudy water vapor map (Left), Cloud Map (Right)

Overlaying the cloud layer and water vapor map shows that the carried out algorithm for cloud extraction is not so much sensitive in mixed pixels. Water vapor amount of the edge of clouds was low either. Hence a pixel buffer applied to the cloud layer to avoid the underestimation caused by these wrong pixels in interpolation process.

In this step at first, processed cloud layer of MERIS data was overlaid to the Water vapor layer. Then a 15 pixels neighborhood was utilized to interpolate the central cloudy pixel by non-polluted pixels using weighted distance algorithm (Li, 2005). As central parts of large clouds or inside of the congested clouds may not obey the rule of smooth changes in water vapor amount, cumulus clouds and a more than 40 percent cloudy 15x15 neighborhood window were masked. The masked points of a single image had to be neglected in other images either.

Water vapor differential error map was formed in this stage. Forming of this map was done by subtracting zenith wet delays. Zenith wet delay was calculated for each pixel and according to the Eq.2 as below (Bevis et. al., 1996):

$$ZWD_{wv} = \Pi^{-1}PWV \quad (2)$$

Where ZWD is the zenith wet delay and Π^{-1} could be derived from Eq. 3 (Hanssen, 2001).

$$\Pi^{-1} = 10^{-6} \rho_1 R_v \left(k'_2 + \frac{k_3}{T_m} \right) \quad (3)$$

Where T_m is the mean temperature of the column containing the water vapor and K coefficients are used as the (Smith and Weintraub, 1953)

$$k_1 = 77.6 K hPa^{-1}$$

$$k'_2 = 23.3 K hPa^{-1}$$

$$k_3 = 3.75 \times 10^5 K^2 hPa^{-1}$$

After that the remained interpolated cloudy pixels were taken into account. Additional error was estimated, using Table 1 (Hanssen, 2001):

Cloud Type	LWC [g/m ³]	SRD [mm/Km]
Stratiforms	0.05-0.25	0.1-0.4
Small cumulus	0.5	0.7
Ice Clouds	<0.1	<0.1

Table1: Liquid Water content and Slant range delay of clouds

Note that the congestus clouds were masked due to the lack of the information of water content of such clouds and geometrical depth of the clouds.

QFE (uncorrected from height effects) was used to estimate the air pressure error. As the wind speed low and the area of interest were not so much vast, a central station was chosen to derive the air pressure. Another station was used to validate the amounts. Air pressure amounts were assumed like Table 2 and extracted from Mashhad Meteorological synoptic data.

Parameter	12-09-2005	08-08-2005
Air Pressure (mb)	903.2	894.6

Table 2: QFE amounts of images.

Air pressure zenith delay was calculated from equation 4.

$$ZHD = 10^{-6} k_1 \frac{R_d}{g_m} P_s \quad (3)$$

Where g_m is the local gravity at centre of atmospheric column.

As could be seen, by using the values of Table 2 around 2 centimeter error was derived which is too much high. If a plane fit algorithm is used for flattening this error will be almost removed. But if a calculative method is implemented, this error may be ruined the results.

The total error map is shown in Figure 4.

To implement this map to the interferogram, the Eq.4 was used (Zebker et al, 1997).

$$\Delta\phi = \frac{4\pi}{\lambda} \frac{ZTD}{\cos\theta_i} \quad (4)$$

In this equation, ZTD is the Zenith total delay and θ is the incident angle at each point. A point to point algorithm was implemented to the interferogram for total atmospheric correction.

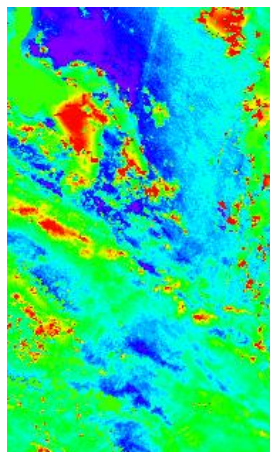


Figure4: Total Error map

For each pixel, the amount of error was extracted by nearest neighbor interpolation of error map and θ was calculated by using the SLC header parameters like near range and height. After implementing the error algorithm, plane fit strategy was chosen to flatten the interferogram. Final Corrected interferogram could be seen in Figure 5.

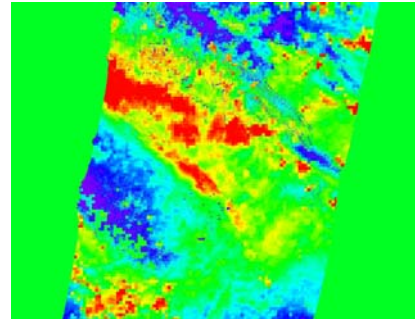


Figure5: Corrected and flattened interferogram

4. RESULTS

GPS time series points were used in this stage to validate the results. 3 points in approximately middle parts of this interferogram and near the subsidence area (where is the research area of interest) was used for this purpose. The distance between the points is around 20 kilometers. The comparison of the values could be seen in Table 3. (The GPS values were obtained from the National Cartographic centre of Iran). The uncertainty of GPS values are around a millimeter.

The total RMS Error of these points is around 8.6 Millimeters which is acceptable in comparison with the other carried out activities.

Points	InSAR (mm)	GPS (mm)
Mashhad	-8	-2
Tous	-52	-41
Torqabeh	5	-3

Table 3: GPS and InSAR deformation

5. CONCLUSION

As it could be seen in validation part and the result map, the atmospheric artifacts was reduced in the correction process. The RMS error of just flattened interferogram was about 1.9 centimeter. Furthermore if the water vapor amounts differed more in location, this error would be intensified.

Implementing the flattening model after atmospheric correction helps the process to obtain better results. By using the flattening model before the correction, some unreal systematic error would be imported to the interferogram; because the specific model which used for flattening will omit the linear errors and linear parts of other influences. This would cause overreduction on the interferogram. Mitigating the air pressure, implementing the total error map to the interferogram and flattening in respect showed around 9.1 millimeters disagreement between InSAR and GPS. This shows that the linear errors like Ionosphere could be neglected if a fit method for flattening was chosen.

Just three points for validation were utilized in this research due to the lack of the GPS facilities in that area. Increasing the GPS points on the InSAR area of research will help the validation be more accurate and even help us to implement new methods like GPS network studies.

In the result map, some remained or weakened artifacts could be seen. These artifacts may exist due to the large pixel size of MERIS reduced resolution products. Some uncertainties in cloud maps shown that, the full resolution product will result in the better final map probably.

ACKNOWLEDGMENTS

This work is supported by K. N. Toosi University of Technology. I expressed my gratitude toward Geological survey of Iran and Iranian space agency for providing image data and consultation. Moreover, I wish to thank to National Cartographic Center for gathering and providing GPS data and Meteorological Organization of Iran for their valuable meteorological data.

REFERENCES

- Bevis, M., S. Chiswell, S. Businger, T.A. Herring and Y. Bock.,1996. Estimation wet delays using numerical weather analysis and predictions, *Radio Science*, 31(3):477-478.
- Davis, J. L., T. A. Herring, I. I. Shapiro, A. E. E. Rogers, and G. Elgered, 1985. Geodesy by radio interferometry: Effects of atmospheric modeling errors on estimates of baseline length, *Radio Sci.*, 20, 1593–1607.
- European Space Agency, MERIS Hand book, Oct.,2006.
- Fischer J., and R. Bennartz. Retrieval of total water vapor content from MERIS Measurements.,MERIS ATBD 2.4. Doc No., PO-TN-MEL-GS-0005, Dec. 1997.
- Hanssen, R.F., 2001. Radar Interferometry: Data interpretation and Error Analysis. Kluwer Academic Publishers, Dordrecht.
- Kramer H.J., Observation of the earth and its environment, Springer, 2002.
- Li, Z., J.-P. Muller, P. Cross, and E. J. Fielding , 2005. Interferometric synthetic aperture radar (InSAR) atmospheric correction: GPS, Moderate Resolution Imaging Spectroradiometer (MODIS), and InSAR integration, *J. Geophys. Res.*, 110, B03410, doi:10.1029/2004JB003446.
- Massonnet, D., M. Rossi, C. Carmona, F. Adragna, G. Peltzer, K. Feigl, and T. Rabaute, 1993. The displacement field of the Landers earthquake, *Nature*, 364, 138–142.
- Mobasheri M.R. Concept of physics in Remote sensing. Publisher: K.N.Toosi University of Technology. 2006.
- Smith, E.K., and S. Weintraub, 1953. The constants in the equation for atmospheric refractive index at radio frequencies, *Proc. IRE*, 41,1035-1037.
- Zebker, H.A., C.L. Werner, P.Rosen and S. Hansley, 1994a. Accuracy of topographic maps derived from ERS-1 radar interferometry, *IEEE Trans. Geosci. Remote Sens.*, 32(4), 823-836.
- Zebker, H.A., P.A. Rosen, R.M. Goldstein, G. Andrew, and C.L., 1994b. Werner, On the derivation of coseismic displacement fields using differential radar interferometry: The Landers earthquake, *J. Geophys. Res.*, 99, 19,617–19,634.
- Zebker, H.A., P.A. Rosen, and S. Hensley, 1997. Atmospheric Effects in Interferometric Synthetic Aperture Radar Surface Deformation and Topographic Maps, *J. Geophys. Res.*, 102(B4), p.7547-7563.

